Available online at www.sciencedirect.com
SCIENCE DIRECT®
ELSEVIER
International Journal of Solids and Structures 42 (2005) 5441–5459
INTERNATIONAL JOURNAL OF SOLIDS and STRUCTURES
www.elsevier.com/locate/ijsolstr

# Study of the antiplane deformation of linear 2-D polycrystals with different microstructures

R.A. Lebensohn [a,*], O. Castelnau [b], R. Brenner [b], P. Gilormini [c]

[a] *Materials Science and Technology Division, Los Alamos National Laboratory, Los Alamos, NM 87845, USA*
[b] *LPMTM (CNRS-UPR9001), Institut Galilée, Université Paris Nord, av. J.B. Clément, F-93430 Villetaneuse, France*
[c] *Laboratoire d'Ingénierie des Matériaux, ENSAM, 151 Bd de l'Hôpital, F-75013 Paris, France*

Received 30 August 2004; received in revised form 18 February 2005
Available online 14 April 2005

**Abstract**

The effective behavior and the distribution of local mechanical fields of linearly viscous 2-D polycrystals under antiplane shear is investigated. Several microstructures are considered, and a full-field approach based on the Fast Fourier Transform technique is applied. First, the accuracy of this technique is evaluated on a strictly isotropic 2-phase microstructure. Voronoi tessellation is then used to generate artificial microstructures, and a real (fully recrystallized) polycrystalline microstructure is obtained by electron back-scattering diffraction. Ensemble averages over several configurations using eight crystalline orientations (phases) are performed. Although a slight anisotropy is obtained for the effective behavior of each individual configuration, statistically, the results are in very good agreement with the available analytical isotropic solution. At phase level, a marked asymmetry is obtained for the distribution of local stresses. The intraphase first- and second-order moments of the stress field, calculated for both microstructures are compared with corresponding self-consistent predictions.
Published by Elsevier Ltd.

*Keywords:* Polycrystals; Antiplane shear; Homogenization; Stress fluctuations

## 1. Introduction

The computation of the mechanical behavior of polycrystalline materials based on their microstructure and the properties of their constituent single-crystal grains is a central problem in materials science. In recent years, the advances in the theories that link microstructures and properties, combined with the

* Corresponding author. Tel.: +1 505 665 3035; fax: +1 505 667 8021.
*E-mail address:* lebenso@lanl.gov (R.A. Lebensohn).

0020-7683/$ - see front matter Published by Elsevier Ltd.
doi:10.1016/j.ijsolstr.2005.02.051

increasing numerical capability of computers, have enabled the development of new concepts and algorithms for predicting the effective response and the local statistics of polycrystals with a given microstructure, and the actual local mechanical fields that appear inside a polycrystal with a particular configuration, as well.

On the one hand, the computation of effective and average local properties is usually accomplished by means of homogenization techniques. This kind of approach provides estimates of the macroscopic mechanical fields in the polycrystal based on statistical information on the distributions of the corresponding quantities at grain level. While for linear polycrystals the self-consistent (SC) model originally proposed by Hershey (1954) delivers very accurate estimates (Kröner, 1958), several SC extensions—based on different linearization schemes—have been proposed for non-linear materials, leading to widely diverging predictions, especially for materials with high non-linearity and strong contrast of properties at single-crystal level. Among these schemes, recent works (Liu and Ponte Castañeda, 2004a,b) based on comparison with bounds showed that the most accurate is the second-order variational formalism of Ponte Castañeda (2002) that takes into account field averages and fluctuations in the grains to define the corresponding linearized behavior at grain level.

On the other hand, the finite element method (FEM) has been applied to obtain full-field solutions for the deformation of a relatively large unit cell or representative volume element (RVE) of elastic polycrystals. This approach has been mainly used to determine the size and number of random RVE configurations needed for an accurate prediction of the effective behavior of random polycrystals, although without paying attention to the distribution of local fields (see Elvin, 1996; Ren and Zheng, 2002 for 2-D polycrystals, and Nygårds, 2003 for 3-D cases). Also, a novel formulation, originally proposed by Moulinec and Suquet (1994, 1998), based on the Fast Fourier Transform (FFT) technique, allows us to obtain a very detailed mapping of the intragranular mechanical fields that appear in a large polycyrstalline RVE, in a very efficient fashion compared with a classical FEM calculation. This full-field solution can be readily used to gather meaningful statistical information at grain and polycrystal levels, and therefore can be used for comparison and cross-validation with SC estimates.

The effective behavior and the distribution of local mechanical fields obtained on several microstructures is the main motivation of the present investigation, that is limited to linearly viscous polycrystals. For this goal, different kinds of microstructures, usually considered to be representative of random polycrystals, will be evaluated using the FFT technique. A relatively simple problem has been chosen, for which a well-known exact solution is available for the effective properties, i.e. the antiplane deformation of a linear random 2-D polycrystal (Dykhne, 1970; Lurie and Cherkaev, 1984). As for the microstructures considered, besides studying here the classical case of ''artificial'' microstructures generated by Voronoi tessellation, one of the novelties of this work consists in the use of the electron back-scattering diffraction (EBSD) technique to obtain a digitalized morphological microstructure of a real (fully recrystallized) polycrystal. This information allows us to assign material properties to the points of a regular grid, as needed for a straightforward implementation of a FFT calculation for this kind of ''real'' microstructure.

The plan of the paper is as follows: in Section 2 we briefly review the 2-D antiplane problem (both the general anisotropic, and the particular isotropic cases) and the Moulinec–Suquet FFT model. In Section 3 we validate the FFT computations by comparison with antiplane analytical results for a rigorously isotropic 2-phase polycrystal, and for a slightly anisotropic polycrystal with square randomly-oriented grains. In the latter case, we also use the concept of *ensemble averages* over different RVE configurations, to obtain the effective properties of random polycrystals using the FFT approach. Next, in Section 3 we apply the above averaging technique to two sets of *8-phase* microstructures, obtained by Voronoi tessellation and by EBSD measurement of a recrystallized copper polycrystal, respectively (note that, in the sequel, the term ''phase'' designates a set of grains with identical mechanical properties, i.e. with the same crystallographic orientation). Effective properties, local stress distributions, and per-phase statistical information for these two microstructures are calculated and compared with SC predictions. Also, a thorough correlation analysis of both microstructures is presented.

## 2. Theory

### 2.1. Antiplane deformation of isotropic 2-D polycrystals: analytical results

Let us consider a model polycrystal consisting of columnar orthorhombic grains with symmetry axes all aligned with the $x_3$ axis, such that, when it is loaded in antiplane mode with shearing direction along $x_3$, the only two slip systems that can be activated in the grains are those defined by the following Schmid tensors

$$\mathbf{m}^{s} = (\mathbf{e}_1 \otimes \mathbf{e}_3 + \mathbf{e}_3 \otimes \mathbf{e}_1)/2, \quad \mathbf{m}^{h} = (\mathbf{e}_2 \otimes \mathbf{e}_3 + \mathbf{e}_3 \otimes \mathbf{e}_2)/2 \tag{1}$$

where $\{\mathbf{e}_1, \mathbf{e}_2, \mathbf{e}_3\}$ is an orthonormal basis of crystallographic axes, and "s" and "h" stand for soft and hard slip systems, respectively. If we further consider that $\mathbf{e}_3$ lies parallel to $x_3$, and if the material is assumed incompressible, the problem becomes two-dimensional. The local stress $\boldsymbol{\sigma}$ and strain rate $\boldsymbol{\varepsilon}$ are characterized by two-dimensional vectors with components $\sigma_{13}$, $\sigma_{23}$ and $\varepsilon_{13}$, $\varepsilon_{23}$ (denoted hereafter $\sigma_1$, $\sigma_2$ and $\varepsilon_1$, $\varepsilon_2$ respectively), and the viscous stiffness tensor, $\mathbf{L} = 2\boldsymbol{\mu}$, by a two-dimensional symmetric second-order tensor with diagonal components equal to $2\mu_{1313}$ and $2\mu_{2323}$, and off-diagonal components equal to $2\mu_{1323}$ (denoted $2\mu_{11}$, $2\mu_{22}$, $2\mu_{12}$ respectively). In addition, the constituent grains exhibit a linear response

$$\boldsymbol{\varepsilon} = \mathbf{L}^{-1} : \boldsymbol{\sigma} = \left( \frac{1}{\tau_0^{s}} \mathbf{m}^{s} \otimes \mathbf{m}^{s} + \frac{1}{\tau_0^{h}} \mathbf{m}^{h} \otimes \mathbf{m}^{h} \right) : \boldsymbol{\sigma}, \tag{2}$$

with $\tau_0^{s}$ and $\tau_0^{h}$ being the viscosities of the soft and hard slip systems (i.e. $\tau_0^{s} < \tau_0^{h}$). Note that in crystal axes $\mu_{11} = \tau_0^{s}$, $\mu_{22} = \tau_0^{h}$, and $\mu_{12} = 0$.

It can be shown that the behavior of such polycrystal is characterized by an effective viscous stiffness tensor $\widetilde{\mathbf{L}} = 2\widetilde{\boldsymbol{\mu}}$, such that $\bar{\boldsymbol{\varepsilon}} = \widetilde{\mathbf{L}}^{-1} : \bar{\boldsymbol{\sigma}}$ (where $\bar{\boldsymbol{\sigma}}$ and $\bar{\boldsymbol{\varepsilon}}$ are the two-dimensional effective stress and strain rate respectively), which obeys (Dykhne, 1970; Lurie and Cherkaev, 1984)

$$\det(\widetilde{\boldsymbol{\mu}}) = \widetilde{\mu}_{11}\widetilde{\mu}_{22} - \widetilde{\mu}_{12}^2 = \tau_0^{s}\tau_0^{h}. \tag{3}$$

In the particular case of an isotropic 2-D polycrystal, $\widetilde{\mu}_{11} = \widetilde{\mu}_{22} (= \widetilde{\mu})$ and $\widetilde{\mu}_{12} = 0$, so that the effective shear modulus $\widetilde{\mu}$ reads

$$\widetilde{\mu} = \sqrt{\tau_0^{s}\tau_0^{h}}. \tag{4}$$

It is worth mentioning that the above result is independent of the 2-D microstructure as far as it remains isotropic. This analytical result will be used below for validating the FFT simulations.

### 2.2. The FFT approach

Moulinec and Suquet (1994, 1998) developed an iterative method based on FFT to compute effective properties and local fields of heterogeneous materials. Lebensohn (2001) used Moulinec–Suquet FFT formulation to compute local fields and texture development of viscoplastic anisotropic 3-D polycrystals. Since the applicability of the original FFT formulation was limited to materials with high rate-sensitivity and low anisotropy, Michel et al. (2000) proposed an improved FFT formulation for composites with high contrast of properties between phases, based on an augmented Lagrangian method. Lebensohn et al. (2004a) used Michel et al. (2000) formulation to deal with antiplane deformation of 2-D power-law polycrystals. In the present problem of linear 2-D polycrystals, either version of the FFT formulation could be used. We chose the improved Michel et al. (2000) formulation, since it is more robust and faster to converge.

Briefly, the FFT formulation is based on the solution of a unit cell problem with periodic boundary conditions, and the augmented Lagrangian method essentially consists in finding a strain rate field, associated

with a kinematically admissible velocity field, that minimizes the average of local work rate, under the constraint imposed by the strain compatibility condition. For this, given that the local mechanical response of an heterogeneous medium can be calculated as a convolution integral between an appropriate Green function and the actual stress heterogeneity (or *polarization*) field, and since such kind of integrals reduces to a simple product in Fourier space, the FFT algorithm is used to transform the polarization field into Fourier space and, in turn, to get the mechanical fields by antitransforming the aforementioned product back to real space. However, since the polarization depends precisely on the a priori unknown mechanical fields, an iterative scheme should be implemented to obtain a consistent full-field solution. For a more detailed description of the algorithms and equations involved, see Michel et al. (2000) and Lebensohn et al. (2004a).

In the present 2-D case, the unit cell should be discretized into a $N_1 \times N_2$ regular array of Fourier points. Each point belongs to a given grain and therefore has associated a given crystallographic orientation (note that in the present 2-D problem, such orientation is fully determined by only one angle, e.g. the angle between the crystallographic axis $\mathbf{e}_1$ and one fixed direction in the plane perpendicular to $x_3$). The dimension of the above grid should be large enough such that each grain is represented by a large number of Fourier points. The FFT solution gives the values of the stress and the velocity gradient in each Fourier point and therefore allows us to compute the corresponding averages and field fluctuations in each grain. Moreover, the polycrystal's effective stress and strain rate can be readily obtained by averaging the corresponding local magnitudes over the entire unit cell.

## 3. Comparison to analytical results

### 3.1. Rigorously isotropic 2-phase case

Numerical results obtained with the FFT formulation will be first compared with analytical expressions available in the case of a linear isotropic 2-D material under antiplane deformation. For this, we need to consider a microstructure such that all possible sources of anisotropy are prevented. These sources of anisotropy can be of the following kinds: (a) *orientational*: if the distribution of orientations (crystallographic texture) is such that, on average, softer crystal directions lie along a particular sample direction; (b) *morphological*: if the grain shape (morphological texture) is such that, on average, the grain axes are longer in one particular sample direction; (c) *topological*: if the local textures of the neighborhood of a given orientation exhibit, in average, orientational or morphological anisotropy. In order to avoid these sources of anisotropy, let us consider the periodic two-dimensional, 2-phase composite shown in Fig. 1, whose unit

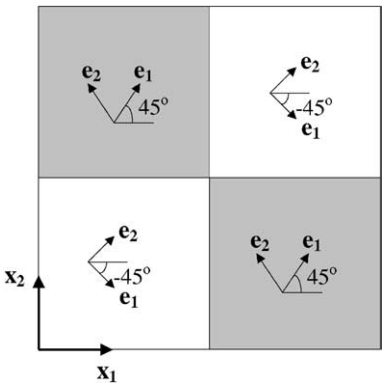


Fig. 1. Two-dimensional 2-phase isotropic unit cell.

cell consists of four square grains, with the crystallographic orientations of the two pairs of opposite grains (i.e. each pair shearing only the central vertex) being characterized by angles +45° and −45°, respectively (note that the orientation of each 2-D crystal is given by the angle between the crystal direction $\mathbf{e}_1$ and the sample direction $x_1$). Such microstructure should provide a strict isotropic response due to the following facts: the 2-D crystallographic and morphologic textures are isotropic, since both have 4-fold symmetry (Milton, 2002), and the neighborhood associated with each grain—i.e. a "chessboard" design, consisting of the alternation of the two types of grains present in the polycrystal—is, in itself, crystallographically and morphologically isotropic.

The antiplane problem for this unit cell has been solved numerically using different numbers of discretization points: 64, 128 and 256 Fourier points along each direction (i.e. 1024, 4096 and 16,384 Fourier points per grain) and two different contrasts: $\tau_0^{\mathrm{h}}/\tau_0^{\mathrm{s}} = 9$ and $\tau_0^{\mathrm{h}}/\tau_0^{\mathrm{s}} = 25$, which give theoretical polycrystal viscosities of $\widetilde{\mu}/\tau_0^{\mathrm{s}} = 3$ and $\widetilde{\mu}/\tau_0^{\mathrm{s}} = 5$, respectively (see Eq. (4)). Fig. 2 shows the relative deviations of the polycrystal viscosities calculated with the FFT model from theoretical values, as the number of iterations of the FFT method increases. It is seen that: (a) the convergence of $\widetilde{\mu}^{\mathrm{FFT}}$ towards its theoretical value is rather good, although it saturates at different levels, depending on the contrast $\tau_0^{\mathrm{h}}/\tau_0^{\mathrm{s}}$ and the number of discretization points used; (b) the precision of the FFT solution can be increased by refining appropriately the Fourier grid. This is due to the fact that a more refined grid provides a higher spatial resolution to represent the rapid fluctuations of the local fields, localized at grain boundaries; (c) higher contrasts require more iterations to achieve the same precision. In any case, the agreement between FFT predictions and theoretical values is satisfactory at the macroscale.

On the other hand, since one of our goals is to understand the influence of the microstructure on the distribution of the stress and strain rate fields, it is important to assess the precision of the FFT results also at local scale. In this context, a great advantage of microstructures with only two phases is that the phase averages of the *localization tensors* $\mathbf{A}$ and $\mathbf{B}$, defined by the expressions $\boldsymbol{\varepsilon}(\mathbf{x}) = \mathbf{A}(\mathbf{x})$: $\bar{\boldsymbol{\varepsilon}}$ and $\boldsymbol{\sigma}(\mathbf{x}) = \mathbf{B}(\mathbf{x})$: $\bar{\boldsymbol{\sigma}}$, can be easily calculated analytically as

$$\begin{aligned} \langle \mathbf{A} \rangle_1 &= \frac{1}{c_1} (\mathbf{L}_1 - \mathbf{L}_2)^{-1} : (\widetilde{\mathbf{L}} - \mathbf{L}_2) \\ \langle \mathbf{B} \rangle_1 &= \frac{1}{c_1} (\mathbf{M}_1 - \mathbf{M}_2)^{-1} : (\widetilde{\mathbf{M}} - \mathbf{M}_2) \end{aligned} \tag{5}$$

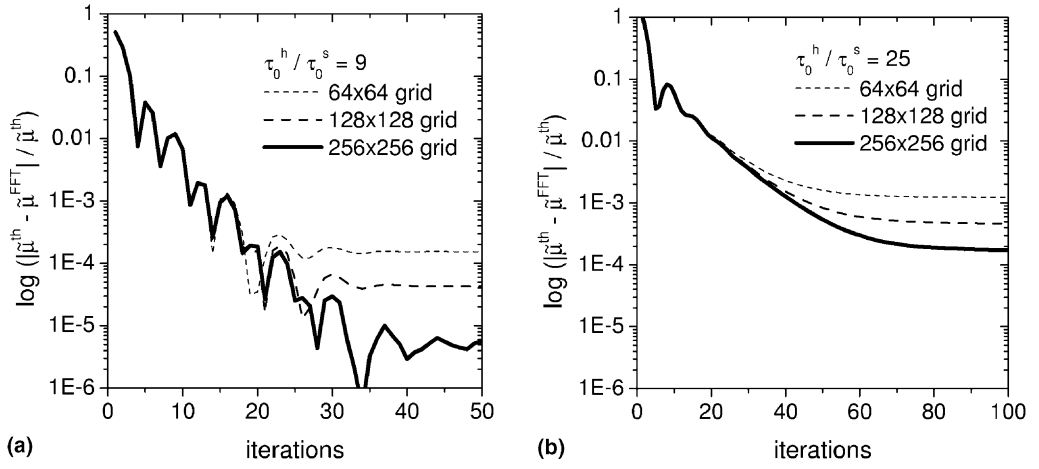


Fig. 2. Relative deviations of polycrystal viscosity predicted with the present formulation (FFT) from theoretical (th) values, in the case of the isotropic RVE of Fig. 1. Cases of (a) $\tau_0^{\mathrm{h}}/\tau_0^{\mathrm{s}} = 9$ ($\widetilde{\mu}/\tau_0^{\mathrm{s}} = 3$) and (b) $\tau_0^{\mathrm{h}}/\tau_0^{\mathrm{s}} = 25$ ($\widetilde{\mu}/\tau_0^{\mathrm{s}} = 5$).

where $c_i$ and $\langle\cdot\rangle_i$ denote volume fraction and average over phase $i = 1,2$, respectively, and the local and effective compliance tensors are given by $\mathbf{M}_i = \mathbf{L}_i^{-1}$ and $\widetilde{\mathbf{M}} = \widetilde{\mathbf{L}}^{-1}$, respectively. Obviously, similar relations can be obtained for $\langle\mathbf{A}\rangle_2$ and $\langle\mathbf{B}\rangle_2$ by interchanging the indices 1 and 2. For isotropic microstructures as the one considered here, since $\widetilde{\mathbf{L}}$ is microstructure-independent, the above expressions are also microstructure-independent. Using the simple analytical solution given by Eq. (4), the phase average localization tensors for the considered microstructure—in the $(x_1, x_2)$ reference frame—are given by

$$\langle\mathbf{A}\rangle_1 = \langle\mathbf{B}\rangle_2 = \begin{pmatrix} 1 & a \\ a & 1 \end{pmatrix}, \quad \langle\mathbf{A}\rangle_2 = \langle\mathbf{B}\rangle_1 = \begin{pmatrix} 1 & -a \\ -a & 1 \end{pmatrix} \tag{6}$$

where the indices 1 and 2 were used for phases at angles $+45°$ and $-45°$, respectively, and

$$a = 1 - 2\Big/\left(1 + \sqrt{\tau_0^{\mathrm{h}}/\tau_0^{\mathrm{s}}}\right). \tag{7}$$

The above analytical expressions can be used to evaluate the accuracy reached with the FFT simulations at phase-average level. Table 1 shows the values of $a$ obtained for contrasts $\tau_0^{\mathrm{h}}/\tau_0^{\mathrm{s}} = 9$ and $\tau_0^{\mathrm{h}}/\tau_0^{\mathrm{s}} = 25$, for different grid refinements. The agreement between the FFT predictions and the theoretical values is as good as for the corresponding effective viscosities shown in Fig. 2 and, like before, is better for lower contrasts and more refined Fourier grids.

### 3.2. Polycrystal with randomly-oriented grains

The standard ergodic hypothesis for systems that are stochastic in space allows obtaining the effective properties of such systems by performing a volume average over a single volume element, which should be large enough to be representative of the microstructure considered (Kröner, 1986). With this in mind, let us first consider a periodic 2-D polycrystal, generated by periodic repetition of a unit cell consisting of square grains with randomly chosen orientations, and that this unit cell—consisting of $32 \times 32 = 1024$ grains—is discretized using a $256 \times 256$ Fourier grid, resulting in $8 \times 8 = 64$ Fourier points per grain.

Despite having equiaxed grains with random orientations, it has been observed that the FFT solution of the antiplane deformation of such "tile" microstructures leads, in general, to a slightly non-isotropic response, as also discussed by Kanit et al. (2003) in the case of 2-phase composites. Indeed, it can be checked that this predicted non-isotropic response is physically meaningful, and not an artifact due to numerical inaccuracies of the FFT calculation, by assessing the fulfillment of the anisotropic analytical relation (3). To attain that goal, the different components of the effective viscosity tensor have been obtained by performing two independent calculations imposing $\bar{\boldsymbol{\varepsilon}} = (\bar{\varepsilon}_1, 0)$ and $\bar{\boldsymbol{\varepsilon}} = (0, \bar{\varepsilon}_2)$, respectively. The corresponding values of $\widetilde{\boldsymbol{\mu}}$ components are reported in Table 2. Note that the two independent computations of the off-diagonal components gives exactly the same results up to the 5th digit. Furthermore, the analytical result (3) is recovered with a relative precision better than $10^{-4}$. It is also worth pointing out that this relative

Table 1
Values of parameter $a$ predicted for different contrasts and grid refinements and relative errors calculated with respect to the theoretical values ($a = 0.5$ for $\tau_0^{\mathrm{h}}/\tau_0^{\mathrm{s}} = 9$, and $a = 2/3$ for $\tau_0^{\mathrm{h}}/\tau_0^{\mathrm{s}} = 25$, see Eq. (7))

| Grid | $\tau_0^{\mathrm{h}}/\tau_0^{\mathrm{s}} = 9$ | | $\tau_0^{\mathrm{h}}/\tau_0^{\mathrm{s}} = 25$ | |
|---|---|---|---|---|
| | $a$ | Relative error | $a$ | Relative error |
| $64 \times 64$ | 0.499877 | $2.46 \times 10^{-4}$ | 0.666021 | $9.69 \times 10^{-4}$ |
| $128 \times 128$ | 0.499957 | $0.86 \times 10^{-4}$ | 0.666340 | $4.90 \times 10^{-4}$ |
| $256 \times 256$ | 0.499987 | $0.26 \times 10^{-4}$ | 0.666452 | $1.87 \times 10^{-4}$ |

Table 2
Components of the effective viscosity tensor obtained by FFT for a periodic 2-D "tile" polycrystal with 1024 randomly oriented grains; case of contrast $\tau_0^h/\tau_0^s = 9$

| $\bar{\varepsilon}_1$ imposed | $\bar{\varepsilon}_2$ imposed |
|---|---|
| $\widetilde{\mu}_{11}/\tau_0^s = 3.08669$ | $\widetilde{\mu}_{22}/\tau_0^s = 2.91638$ |
| $\widetilde{\mu}_{21}/\tau_0^s = -0.03435$ | $\widetilde{\mu}_{12}/\tau_0^s = -0.03435$ |

precision—obtained with "only" $8 \times 8$ Fourier points per grains—is better than the one previously obtained for the 2-phase isotropic microstructure with $32 \times 32$ points per grain (see Fig. 2).

It is thus evident that a unit cell of such microstructure and dimensions is not actually representative of the class of isotropic polycrystals with random microstructure. For this, it would be necessary to consider a very large volume element, containing a large number of different grains, some of them with the same orientation but different environments. The size of a unit cell and the corresponding Fourier grid that would fulfill the above condition—while keeping a large number of Fourier points inside each grain to capture intragranular heterogeneities—would require numerical capabilities far beyond standard available resources.

Another way of obtaining effective properties of stochastic systems without need of large representative volume elements, is by performing ensemble averages, i.e. averages over the outcomes of simulations performed on many specimens, randomly generated (Sab, 1992; Kanit et al., 2003; Moulinec and Suquet, 2003; Lebensohn et al., 2004a). With this in mind, Fig. 3 shows the distributions of $\widetilde{\mu}_{11}/\tau_0^s$ and $\widetilde{\mu}_{21}/\tau_0^s$, obtained for 100 configurations of the "tile" unit cell described above, and for $\tau_0^h/\tau_0^s = 9$. While the ensemble averages $\overline{\widetilde{\mu}}_{11}/\tau_0^s$ and $\overline{\widetilde{\mu}}_{21}/\tau_0^s$ of the viscosity components deviate less than 0.5% from the theoretical values, a relatively large dispersion is observed for each individual configuration, as indicated by the corresponding standard deviations (SD).

The above example confirms the difficulty of constructing an isotropic 2-D polycrystal of that size by choosing *randomly* the crystalline orientations, even in the case of the "tile" microstructure where the morphology and the volume fraction of the individual grains have been fixed in advance (and not randomly chosen, as in the case of more general random microstructures).

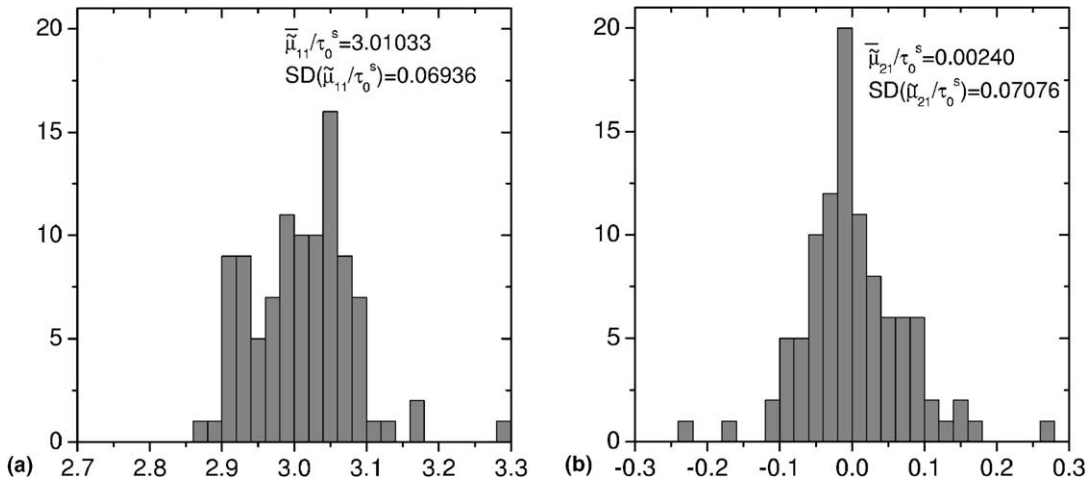


Fig. 3. Distributions of (a) $\widetilde{\mu}_{11}/\tau_0^s$ and (b) $\widetilde{\mu}_{21}/\tau_0^s$ for 100 randomly generated configurations of the "tile" unit cell (1024 grains, $\tau_0^h/\tau_0^s = 9$). Mean values and standard deviations (SD) are indicated.

## 4. Application to 8-phase polycrystals

### 4.1. Description of the microstructures

The former examples motivate the following question: is it possible to construct volume elements, of similar size as above, having relatively complex microstructures, while exhibiting the less possible anisotropic behavior? One way of eliminating the orientational anisotropy and, at the same time, minimizing the topological anisotropy is by reducing the number of orientations to the minimum possible, taking them regularly spaced, instead of choosing them randomly. In doing this, and for reasons that will become evident in the sequel, we have worked with eight symmetric crystallographic orientations, determined by the angles 0°, 22.5°, 45°, 67.5°, 90°, 112.5°, 135°, and 157.5°. Hence, for every microstructure considered, we have assigned to its "grains" (i.e. simply connected domains with the same orientation) one of the eight orientations above. This assignation has been at random, under the constraint that, upon completion, (a) the volume fractions of the eight "phases" (i.e. sets of grains having the same orientation) should be equal, and (b) two neighbour grains do not belong to the same phase. In what follows, ensemble averages over several of such configurations, for effective and local quantities, will be calculated. It is important to mention that the same morphology has been considered for the generation of the different configurations, varying thus only the topology. In that sense, the considered microstructures present only a *restricted random* character. Generating real random microstructures would lead to different phase volume fraction, morphology and topology, for each configuration (Kanit et al., 2003). The main justification of our choice is to decrease the number of configurations that should be averaged to obtain a strict isotropic ensemble response. This restricted random procedure guarantees, on the one hand, orientational isotropy and, on the other hand, allows grains of the same orientation to be surrounded by many different environments, something that should contribute to minimize the anisotropy of topological origin. Furthermore, the choice of eight phases with those particular orientations has some merits:

(a) since the application of the FFT algorithm requires the number of Fourier points (i.e. *pixels*) along each direction $(N_1, N_2)$ to be powers of two, the fact that the total number of pixels is divisible by eight allows for the assignation of identical volume fraction to each phase;
(b) the assignation of one orientation to each grain, under the constraint that such orientation should be different from the ones of every neighbor grain, can be easily achieved with eight phases. Indeed, the minimum number of "colors" (i.e. phases) needed to fill a 2-D image is four (Appel and Haken, 1977);
(c) according to their orientation with respect to the applied deformation, it is possible to identify a *soft* phase (0°), a *medium* phase (e.g. 45°) and a *hard* phase (90°). This classification will be relevant to the discussion of the local stress distributions (see Section 4.4).

In what follows, we show results of such kind of 8-phase polycrystals, for two different microstructures : (a) an "artificial" one, generated by Voronoi tessellation and (b) a "real" one, measured on a recrystallized copper sample.

#### 4.1.1. The "Voronoi" microstructure

The first microstructure considered here is a periodic unit cell generated by Voronoi tessellation. Since a FFT calculation requires a discrete description of the microstructure on a regularly-spaced grid over the RVE, the procedure is simpler than in the case of having to determine the exact position of the boundaries between Voronoi cells in a continuum. We have proceeded as follows: (a) 8500 points were randomly distributed in a square unit cell; this Poisson distribution of points constitutes the nuclei of the random grains; (b) the sides of the RVE were divided into equispaced 512 points, determining a $512 \times 512$ regular Fourier grid; (c) each Fourier point was assigned to its nearest nucleus (taking into account periodic boundary con-

ditions across the RVE limits) determining 8500 different domains (grains). In turn, this basic *morphological* microstructure was used to generate 50 different *topological* configurations of the 8-phase polycrystal described above, by randomly assigning to each of the 8500 grains one of the eight symmetric orientations listed earlier. Fig. 4(a) shows a typical 8-phase "Voronoi" microstructure.

It is worth situating the above procedure in the context of other generation schemes for random microstructures. A random polycrystal is a prototypical example of a *cellular* microstructure, obtained by partitioning the space into space-filling cells (i.e. grains) (Torquato, 2002). Different Voronoi microstructures can be obtained according to the way in which the points that serve as a basis for tessellation are distributed. If the random points have a Poisson distribution, the resulting microstructure can have arbitrarily small grains. If this is to be avoided, the distance between random points should be limited by a minimum distance, as in the case of the *hard core model* and its variants (Buryachenko et al., 2003), which, in another context, correspond to a random dispersion of impenetrable spheres (Torquato, 2002). In our case, due to the specific Fourier discretization required to apply the FFT formulation, the resulting Voronoi microstructure can be thought as a mix of both aforementioned models. While the random points have a Poisson distribution, the finite size of the step of the Fourier grid (i.e. the distance between two consecutive pixels) guarantees that the smallest grains have an area of at least one Fourier step by one Fourier step (i.e. comprising one pixel).

#### *4.1.2. The recrystallized copper ("ReX Cu") microstructure*

The second microstructure of interest is the one of a fully recrystallized copper polycrystal. The copper sample has been cold rolled (83% thickness reduction) then thermally treated (15 min at 300 °C) to achieve complete recrystallization. The resulting morphology of such process shows equiaxed grains and can be measured by EBSD under scanning electron microscopy (SEM). The advantage of this technique, besides its high spatial resolution, is that it directly provides an image of the microstructure that can be digitalized over a square regular grid, and used directly to perform the FFT simulations.

The crystallographic orientations of the copper grains are obtained by the EBSD technique, so that the grain boundaries can be easily located. This results in a digitalized microstructure of $512 \times 512$ pixels, each pixel being indexed with a number that identifies the grain to which it belongs. The total number of such grains was 8697, i.e. similar to the "Voronoi" microstructure described above. For our purpose, the actual

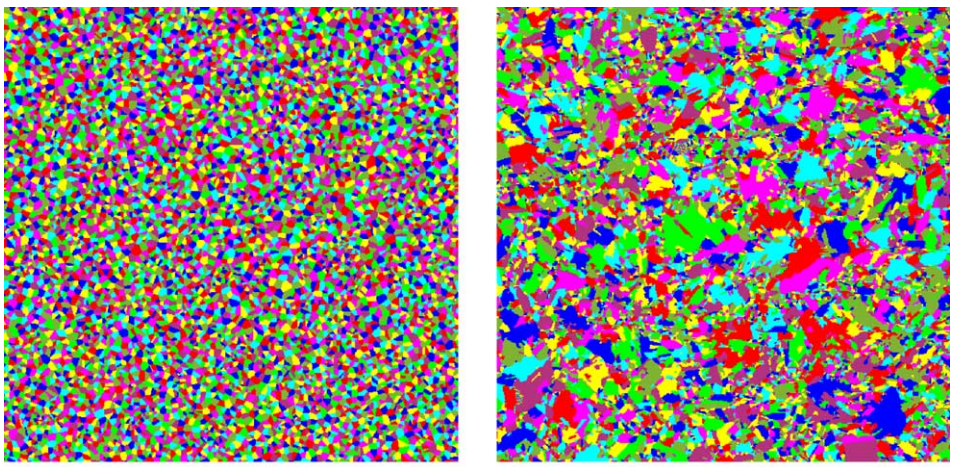


Fig. 4. Typical (a) "Voronoi" and (b)"ReX Cu" microstructures.

grain orientations were not further used, only the measured morphology was retained. Then, like in the "Voronoi" case, this morphological microstructure was used to randomly generate 50 different topological 8-phase polycrystal configurations. Fig. 4(b) shows a typical 8-phase "ReX Cu" microstructure.

It is worth noting that, unlike in the "Voronoi" case (in which it was possible, during the generation of the basic microstructure, to impose periodic boundary conditions and therefore obtain a smooth transition through RVE boundaries), in the present case, the periodic polycrystals generated from the 2-D image exhibit changes from grains located inside the unit cell to other (completely decorrelated) grains located across the RVE boundary. One possible remedy to this lack of actual periodicity across the RVE would have been to introduce slight changes in the properties of the points near the RVE boundary to enforce a smooth transition from the inside to the outside of the unit cell, i.e. an imaging technique called *morphing*. This, however, was not necessary in our case, since the influence of those spurious grain boundaries on the predicted effective and local response was minimal. To start with, these boundaries are not too sharp, since the mechanical contrast across the RVE boundary remains the same as it is inside the unit cell across actual grain boundaries. Moreover, the present problem exhibits a clear *scale separation*, i.e. the RVE size is much larger than the average heterogeneity size. Therefore, the width of the region affected by the presence of those artificial grain boundaries is expected to be only a few times the average heterogeneity size. To illustrate this, we have slightly modified the morphologic microstructure measured by EBSD by replacing an outer rim of the RVE of 11 pixels width (i.e. 2 times the average grain size given by $\sqrt{(512 \times 512)/8697} \approx 5.5$ pixels) by an isotropic material whose behavior was forced to be strictly the expected macroscopic one, given by Eqs. (3) and (4). Comparing the response of both microstructures, the effective viscosities differ in less than 0.03%, while the average difference in the local mechanical fields over the whole polycrystal is less than 0.5%.

### 4.2. Effective behavior

The calculated response under antiplane loading of the two sets of 2-D microstructures is now described. Fig. 5(a) and (b) show the distributions of polycrystal viscosities $\widetilde{\mu}_{11}/\tau_0^s$ and $\widetilde{\mu}_{21}/\tau_0^s$, for 50 configurations of the "Voronoi" microstructure with $\tau_0^h/\tau_0^s = 9$. Evidently, the reduction to only eight symmetric phases and the random procedures followed to construct this microstructure, were not enough to prevent a slight non-isotropic behavior of each individual configuration. However, the comparison between these results and the former "tile" unit cell distributions (see Fig. 3) shows that: (a) in the "Voronoi" case, the average viscosities $\widetilde{\bar{\mu}}_{11}/\tau_0^s$ and $\widetilde{\bar{\mu}}_{21}/\tau_0^s$ are roughly one order of magnitude closer to the isotropic analytical results than those of the "tile" case, even though they correspond to half the number of configurations, and (b) the dispersions of the "Voronoi" distributions are significantly smaller than in the "tile" case.

Fig. 5(c) and (d) show the same results for the "ReX Cu" microstructure. In this case, it can be observed that: (a) the mean values of the "ReX Cu" distributions exhibit similar deviations from theoretical values than those of the "Voronoi" distributions, and (b) the dispersions are higher in the "ReX Cu" case than in the "Voronoi" case.

To assess more quantitatively the significance of these results, it is interesting to estimate the error that can be associated with the above ensemble averages. For any statistically distributed quantity $f$, the mean value over a given distribution provides only an estimate of the expectation $\mathbb{E}(f)$, such that

$$\mathbb{E}(f) \approx \frac{1}{N_\alpha} \sum_{i=1}^{N_\alpha} f^\alpha \pm \frac{\mathrm{SD}(f)}{\sqrt{N_\alpha}} \tag{8}$$

where $N_\alpha$ is the number of configurations. In this connection, Table 3 shows a comparison between the *statistical uncertainty* $\mathrm{SD}(\cdot)/\sqrt{N_\alpha}$ and the distance between the theoretical and calculated (average) viscosities, in the "Voronoi" and "ReX Cu" cases. It can be seen that, in both cases, the distance between the

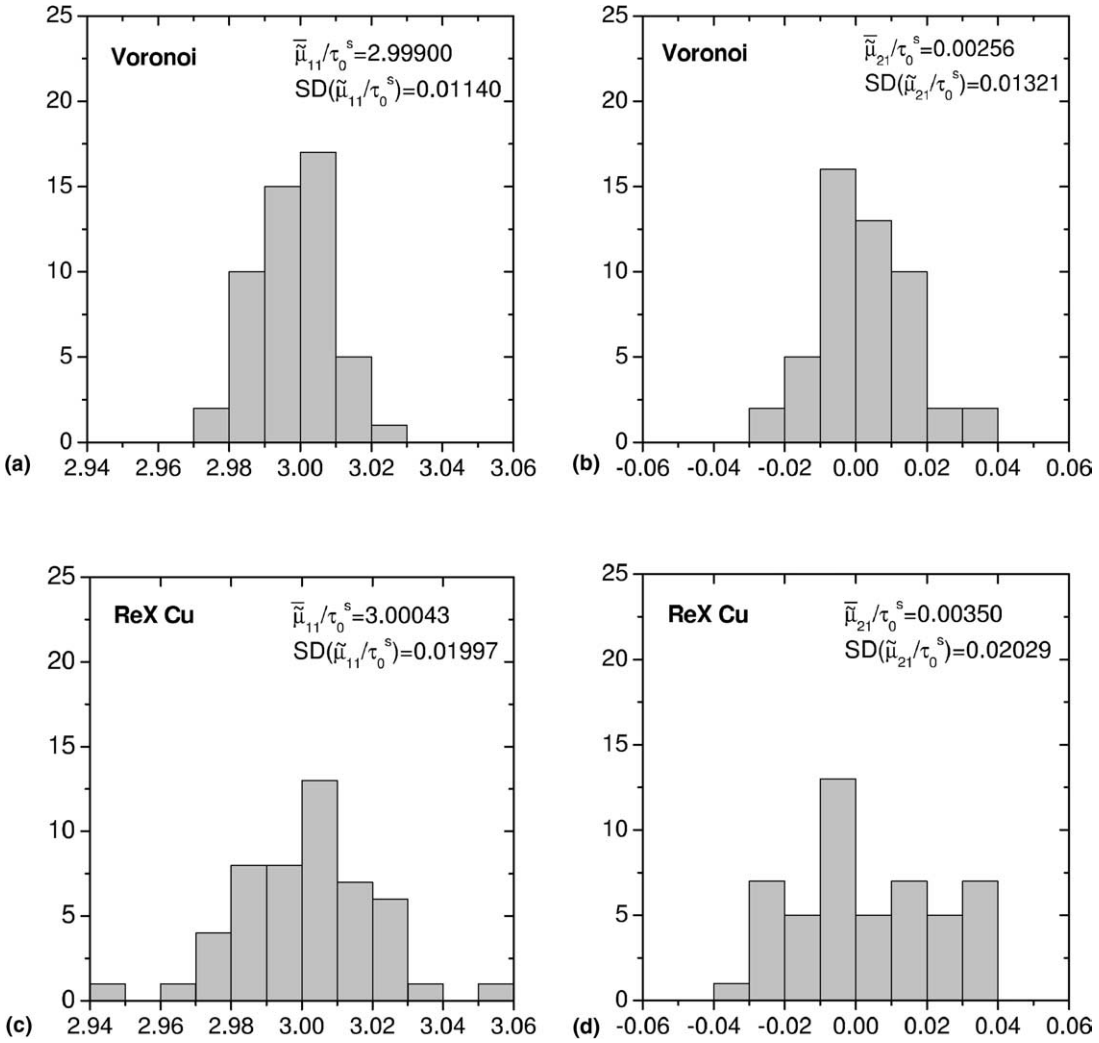


Fig. 5. Distributions of $\tilde{\mu}_{11}/\tau_0^s$ and $\tilde{\mu}_{21}/\tau_0^s$, for 50 configurations of: (a, b) "Voronoi" and (c, d) "ReX Cu" microstructures (contrast: $\tau_0^h/\tau_0^s = 9$).

Table 3
Distance between theoretical and calculated viscosities, and statistical uncertainty (see Eq. (8), for 50 configurations, in the "Voronoi" and "ReX Cu" cases)

| | $\left\lvert \frac{\bar{\tilde{\mu}}_{11} - \tilde{\mu}_{11}^{th}}{\tau_0^s} \right\rvert$ | $\frac{SD(\tilde{\mu}_{11}/\tau_0^s)}{\sqrt{N_\alpha}}$ | $\left\lvert \frac{\bar{\tilde{\mu}}_{21} - \tilde{\mu}_{21}^{th}}{\tau_0^s} \right\rvert$ | $\frac{SD(\tilde{\mu}_{21}/\tau_0^s)}{\sqrt{N_\alpha}}$ |
|---|---|---|---|---|
| Voronoi | 0.00100 | 0.00161 | 0.00256 | 0.00187 |
| Rex Cu | 0.00043 | 0.00282 | 0.00350 | 0.00287 |

theoretical and the calculated diagonal component of the viscosity is of the same order and smaller than the corresponding statistical uncertainty, while for the off-diagonal component it is slightly higher. These results thus suggest that the ensemble averages match with the theoretical values, within the statistical errors associated with the averaging procedure.

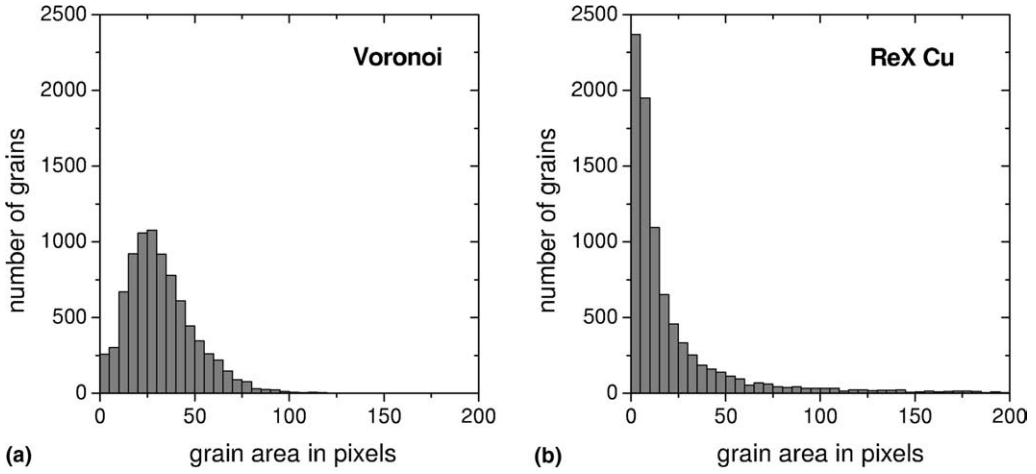


Fig. 6. Grain size distributions of: (a) "Voronoi" and (b) "ReX Cu" microstructures.

Concerning the comparison between both microstructures, the different grain size distributions (Fig. 6) can explain the higher dispersion of the "ReX Cu" results. While the maximum grain area in the "Voronoi" case is 145 pixels, in the "ReX Cu" microstructure the biggest grain has as many as 2646 pixels. These very large grains have a large number of neighbouring grains (up to 82), unlike the "Voronoi" case, in which the number of neighbours does not exceed 12. Moreover, the "ReX Cu" microstructure has a larger fraction of small grains, inside which the field gradients are expected to be higher than in larger grains. Due to these rapidly changing fields, larger numerical inaccuracies are expected to occur in the "ReX Cu" than in the "Voronoi" case, for the same Fourier discretization.

### 4.3. Correlation analysis of the microstructures

An efficient way to estimate quantitatively the deviation from topological isotropy is to calculate the correlation function of the microstructures. Here, we restrict the analysis to correlation functions up to order 2 because it is sufficient for our purpose. Let us call $\chi_r$ the characteristic function of the microstructure, i.e. $\chi_r(\mathbf{x}) = 1$ if position $\mathbf{x}$ belongs to phase $r$ and $\chi_r(\mathbf{x}) = 0$ otherwise. The 2-point correlation function (covariance) $C_{rs}$ is defined by

$$C_{rs}(\mathbf{h}) = \langle \chi_r(\mathbf{x}) \chi_s(\mathbf{x}+\mathbf{h}) \rangle \tag{9}$$

with $\langle \cdot \rangle$ denoting the average over the whole microstructure area. Note that, in the above definition, $C_{rs}$ only depends on the relative position $\mathbf{h}$ due to the stationarity of the microstructure that results from the random generation process described above. The correlation functions are generally not symmetric but obey

$$C_{rs}(\mathbf{h}) = C_{sr}(-\mathbf{h}) \tag{10}$$

except for 2-phase materials for which $C_{rs}(\mathbf{h}) = C_{rs}(-\mathbf{h})$ due to the general property

$$\sum_{r=1}^{n} C_{rs}(\mathbf{h}) = \sum_{r=1}^{n} C_{sr}(\mathbf{h}) = c_s \quad \forall \mathbf{h} \tag{11}$$

$n$ being the number of phases and $c_s = \langle \chi_s \rangle$ the volume fraction of phase $s$. Accordingly, there are only $n(n-1)/2$ independent covariances. The relation

$$C_{rs}(\mathbf{0}) = c_r \delta_{rs} \tag{12}$$

($\delta_{rs}$ is the Kronecker symbol) is general, but the other classical limit

$$\lim_{\|\mathbf{h}\| \to \infty} C_{rs}(\mathbf{h}) = c_r c_s \tag{13}$$

only holds if there is no order at large distance, which is not the case considered here, owing to the periodicity of the microstructures. However, this limit should be attained at distances $\|\mathbf{h}\|$ larger than the grain size and smaller than the size of the considered configuration if there is no specific order within the configuration, and if this configuration is large enough with respect to the grain size (Bornert, 2001).

With $n = 8$, the 28 independent covariances were obtained by calculating the $C_{rs}$ for $s \leqslant r < n$. The results, calculated for the morphological configurations shown in Fig. 4, are given in Fig. 7 for $\mathbf{h}$ pointing along $x_1$ and along $x_2$. In order to preserve consistency with the FFT approach, calculations have been performed accounting for the microstructure periodicity, i.e. applying the classical toroidal edge correction, e.g. see Buryachenko et al. (2003). Here, since there is no particular symmetry in the considered microstructures due to their random character, global isotropy can be achieved only if there is no directionality in the topology and the morphology. That is, all phases must be on the same footing, i.e. all $C_{rs}$ ($r \neq s$) and all $C_{rr}$ must be respectively superimposed. According to Fig. 7, these conditions are not exactly met for the two microstructures. However, less anisotropy is expected for the "Voronoi" case, and this may explain the smaller standard deviations on the effective viscosity observed for this microstructure (see Fig. 5). The slower decrease of the auto-correlations $C_{rr}$ indicates a larger characteristic length (the distance at which

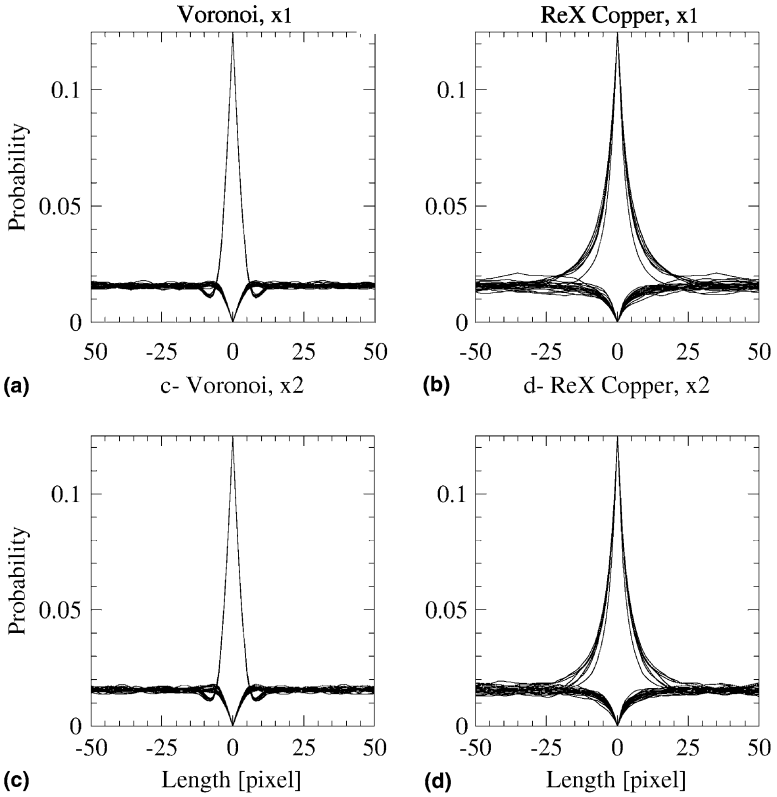


Fig. 7. The 28 independent covariances $C_{rs}$ (i.e. for $s \leqslant r < 8$) obtained for a single realization of the "Voronoi" and "ReX Cu" microstructures, along the $x_1$ and $x_2$ directions.

$C_{rr} = c_r^2$) of about 35 pixels for the "ReX Cu", whereas it is only about 6 pixels for the "Voronoi" microstructure. The latter value matches closely the average grain size (≈5.5 pixels) associated with a smaller spread in the grain size distribution (see Fig. 6).

For a better assessment of the morphological anisotropy, the ensemble averages of the covariances over the 50 topological configurations are shown in Fig. 8. Now, the results obtained along four independent directions are superimposed, so that each figure contains $28 \times 4 = 112$ plots. While the almost perfect isotropy of the "Voronoi" morphology is evident, not so good results are obtained for the "ReX Cu". However, recalling that the latter microstructure comes from a real material that was subjected to severe plastic deformation and heat treatments, such a low level of morphological anisotropy was in fact not really expected.

The above correlation analysis explains the larger deviations from theoretical effective viscosities observed in the "ReX Cu" case (see Fig. 5). It is however probable that at least a portion of this higher dispersion can be ascribed to numerical inaccuracies linked to the presence of very small grains and to the fact that the RVE limits are also grain boundaries.

### 4.4. Local stress distribution

Besides the prediction of effective properties, the FFT method also gives relevant information on the field heterogeneity at local level. Figs. 9 and 10 show (for $\tau_0^h/\tau_0^s = 9$) the distributions of local equivalent stresses (normalized with the ensemble average macroscopic equivalent stress $\bar{\sigma}_{eq}$) in a soft phase (at 0°), a medium phase (at 45°) and a hard phase (at 90°), for 1 and 50 "Voronoi" and "ReX Cu" configurations (note that these distributions consist in a large number of Fourier points per phase, i.e. 32,768 and 1,638,400 for 1 and 50 configurations respectively). In the present 2-D antiplane case, the von Mises equivalent stress is defined by $\sigma_{eq} = \sqrt{3}(\sigma_1^2 + \sigma_2^2)^{1/2}$.

In both cases, it can be seen that the distributions for 1 and 50 configurations are almost identical. Moreover, it has been verified over several configurations of both microstructures that each single distribution behaves almost identically. Thus, it can be concluded that the particular topological configuration has a negligible influence on the per-phase stress distribution.

Interestingly, all the histograms of Figs. 9 and 10 (in particular those corresponding to 50 configurations) show some degree of asymmetry, resembling a log-normal rather than a Gaussian distribution, being this asymmetry more marked in the soft phase. This means that the asymmetries *are not* averaged out by the ensemble average procedure. Similar kind of asymmetrical distribution has also been reported by Moulinec

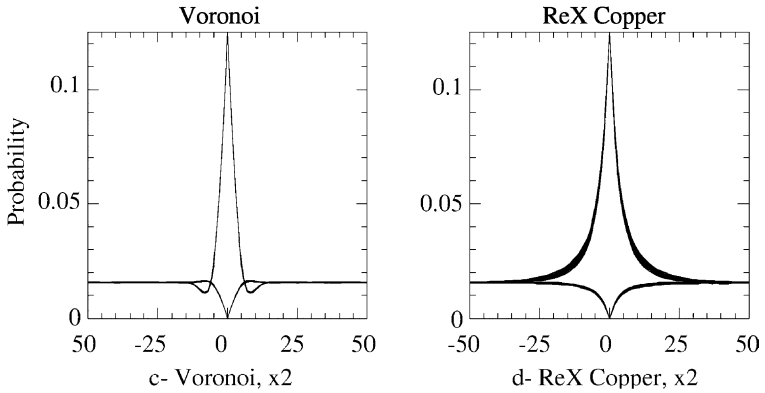


Fig. 8. Ensemble averages over the 50 configurations of the 28 independent covariances $C_{rs}$, $s \leqslant r < 8$, obtained for the "Voronoi" and "ReX Cu" microstructures. In each plot, the $C_{rs}$ calculated along four directions (0°, 45°, 90°, and 135° from $x_1$) are superimposed.

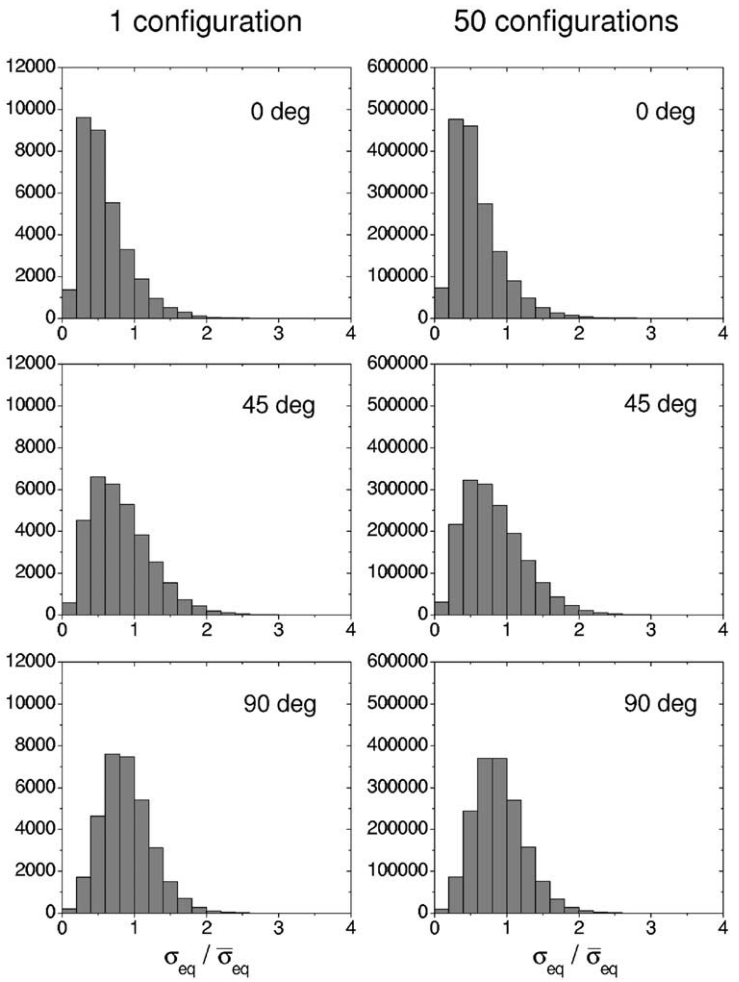


Fig. 9. Distributions of normalized local equivalent stresses for 1 and 50 "Voronoi" configurations, in a soft (0°), a medium (45°) and a hard (90°) phase. Case of $\tau_0^h/\tau_0^s = 9$.

and Suquet (2003) in the case of non-linear two-phase composites, as an evidence of strain localization. It follows that non-vanishing odd higher-order moments of the stress distribution should be expected to develop in the grains of random polycrystals, even in the case of a linear behavior. This important conclusion is relevant to the interpretation of the different available non-linear homogenization procedures, most of them based on information on first-order statistical information, or—in the case of the most recent and accurate ones— on both first- and second-order moments at the grain level (Ponte Castañeda, 2002). According to the above observations, since an asymmetric distribution cannot be fully determined from its first- and second-order moments only, some additional degree of inaccuracy will be necessarily associated to any of the available homogenization schemes for non-linear heterogeneous materials.

### 4.5. Per-phase ensemble averages

For a more qualitative analysis of the FFT results at local level, it is useful to calculate the statistical moments of the above distributions. Our analysis will be focused on the per-phase first- and second-order

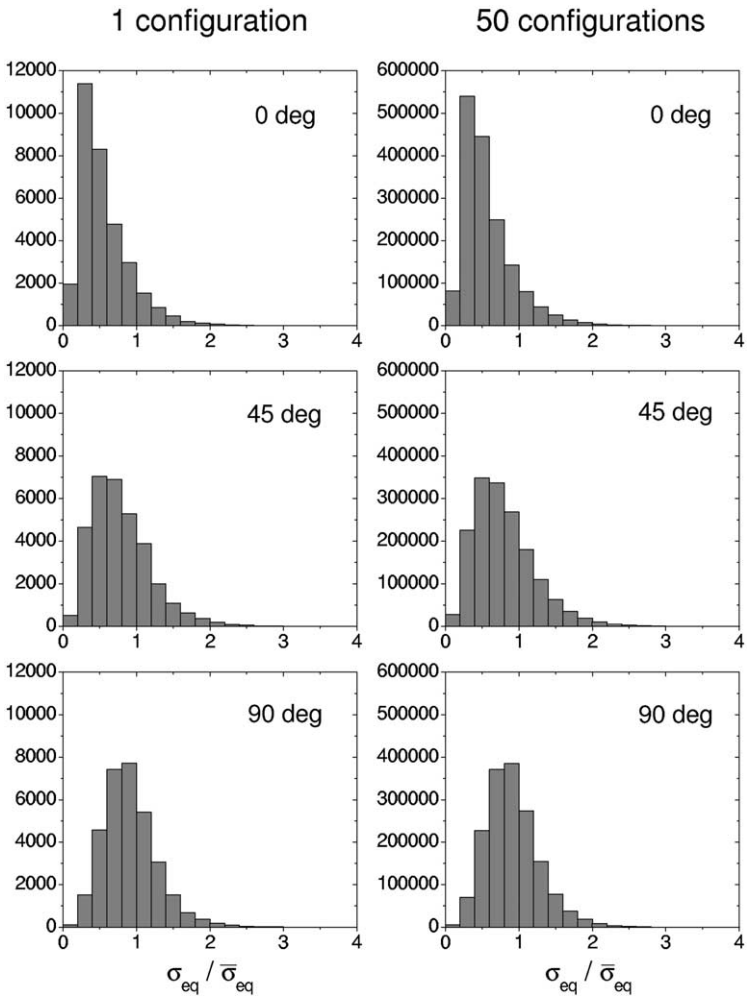


Fig. 10. Distributions of normalized local equivalent stresses for 1 and 50 "ReX Cu" configurations, in a soft (0°), a medium (45°) and a hard (90°) phase. Case of $\tau_0^{\mathrm{h}}/\tau_0^{\mathrm{s}} = 9$.

moments of the stress, that give the mean values and the average stress fluctuations in the phases, respectively. The ensemble averages over $N_\alpha$ configurations of the per-phase first- and second-order moments of the equivalent stress in phase $r$ are calculated as

$$\bar{\sigma}_{\mathrm{eq}}^{r} = \left[\frac{1}{N_\alpha}\sum_{\alpha=1}^{N_\alpha}\langle\boldsymbol{\sigma}\rangle_r^\alpha\right]_{\mathrm{eq}} = \frac{\sqrt{3}}{N_\alpha}\left[\left(\sum_{\alpha=1}^{N_\alpha}\langle\sigma_1\rangle_r^\alpha\right)^2 + \left(\sum_{\alpha=1}^{N_\alpha}\langle\sigma_2\rangle_r^\alpha\right)^2\right]^{1/2} \tag{14}$$

$$\bar{\bar{\sigma}}_{\mathrm{eq}}^{r} = \left(\frac{1}{N_\alpha}\sum_{\alpha=1}^{N_\alpha}\left\langle\sigma_{\mathrm{eq}}^2\right\rangle_r^\alpha\right)^{1/2} = \left(\frac{3}{N_\alpha}\sum_{\alpha=1}^{N_\alpha}\langle\sigma_1^2+\sigma_2^2\rangle_r^\alpha\right)^{1/2} \tag{15}$$

where $\langle\cdot\rangle_r^\alpha$ denotes average over phase $r$ in configuration $\alpha$.

The FFT predictions for the above ensemble average quantities were calculated over 50 configurations, for the "Voronoi" and the "ReX Cu" morphologies. The resulting average first- and second-order moments—normalized with the ensemble average equivalent stress—are shown in Table 4 (4th and 6th columns).

The above FFT estimates can be compared with those obtained by means of the self-consistent (SC) scheme. As shown by Kröner (1978), the linear SC scheme provides the exact solution for so-called *perfectly-disordered* random polycrystals. Such microstructure is characterized by the fact that *all*—i.e. up to infinite order—correlation functions are statistically homogeneous, isotropic, and disordered. Since the corresponding microstructures are different, results from the "Voronoi", "ReX Cu", and perfectly-disordered cases should not necessarily be identical, but comparing them can provide an insight of the effect of the microstructure on the per-phase first- and second-order moments. Following Lebensohn et al. (2004a), who obtained, in the linear 2-D case under consideration, the analytical expressions of the statistical moments, by differentiation of the effective energy (Ponte Castañeda and Suquet, 1998), one can easily derive that the SC estimates of the per-phase first- and second-order moments are given by

$$\frac{\bar{\sigma}^r_{\mathrm{eq}}}{\bar{\sigma}_{\mathrm{eq}}} = \frac{2}{1+\sqrt{M}}\left(1+8\sin^2\theta\right)^{1/2} \tag{16}$$

$$\frac{\bar{\bar{\sigma}}^r_{\mathrm{eq}}}{\bar{\sigma}_{\mathrm{eq}}} = \frac{\sqrt{3}}{1+\sqrt{M}}\left(\frac{\left(\sqrt{M}-1\right)^2}{6\sqrt{M}}(M+1)+\frac{4}{3}\left(1+8\sin^2\theta\right)\right)^{1/2} \tag{17}$$

where $\theta$ is the angle defined in Fig. 1 and $M = \tau_0^{\mathrm{h}}/\tau_0^{\mathrm{s}}$. The 3rd column of Table 4 shows the above SC estimates for comparison with the FFT results. It is seen that the relative differences with respect to those SC estimates (5th and 7th columns) are of the order of $10^{-3}$ or less, and $10^{-2}$, for the "Voronoi" and "ReX Cu" microstructures, respectively. These small relative differences indicate that the ensemble averages over

Table 4
Normalized ensemble averages of 1st and 2nd moments of the equivalent stress predicted with FFT for the "Voronoi" and "ReX Cu" microstructures and relative differences with respect to the corresponding SC estimates; case of contrast $\tau_0^{\mathrm{h}}/\tau_0^{\mathrm{s}} = 9$

| Phase | Moment | SC | Voronoi | Rel. diff. | ReX Cu | Rel. diff. |
|---|---|---|---|---|---|---|
| 0 | 1st | 0.50000 | 0.49939 | $1.4\times10^{-3}$ | 0.48508 | $3.0\times10^{-2}$ |
| | 2nd | 0.81650 | 0.81657 | $0.6\times10^{-3}$ | 0.79551 | $2.7\times10^{-2}$ |
| 22.5 | 1st | 0.73681 | 0.73049 | $6.2\times10^{-3}$ | 0.70719 | $4.4\times10^{-2}$ |
| | 2nd | 0.97957 | 0.97369 | $5.1\times10^{-3}$ | 0.94807 | $3.5\times10^{-2}$ |
| 45 | 1st | 1.11803 | 1.12120 | $4.7\times10^{-3}$ | 1.08563 | $2.9\times10^{-2}$ |
| | 2nd | 1.29099 | 1.29468 | $4.3\times10^{-3}$ | 1.25983 | $2.4\times10^{-2}$ |
| 67.5 | 1st | 1.39897 | 1.40004 | $0.8\times10^{-3}$ | 1.40307 | $0.4\times10^{-2}$ |
| | 2nd | 1.54071 | 1.54222 | $0.8\times10^{-3}$ | 1.54754 | $0.5\times10^{-2}$ |
| 90 | 1st | 1.50000 | 1.49810 | $1.7\times10^{-3}$ | 1.53769 | $2.7\times10^{-2}$ |
| | 2nd | 1.63299 | 1.63041 | $2.0\times10^{-3}$ | 1.67376 | $2.6\times10^{-2}$ |
| 112.5 | 1st | 1.39897 | 1.40105 | $0.4\times10^{-4}$ | 1.42923 | $1.9\times10^{-2}$ |
| | 2nd | 1.54071 | 1.54239 | $1.8\times10^{-4}$ | 1.57353 | $1.9\times10^{-2}$ |
| 135 | 1st | 1.11803 | 1.11819 | $0.9\times10^{-3}$ | 1.10397 | $1.2\times10^{-2}$ |
| | 2nd | 1.29099 | 1.29104 | $0.7\times10^{-3}$ | 1.27926 | $0.8\times10^{-2}$ |
| 157.5 | 1st | 0.73681 | 0.73499 | $3.3\times10^{-3}$ | 0.70641 | $4.1\times10^{-2}$ |
| | 2nd | 0.97957 | 0.97759 | $3.7\times10^{-3}$ | 0.94902 | $3.0\times10^{-2}$ |

the 50 configurations lead to intraphase field averages and fluctuations in very good agreement with the ones predicted by the SC scheme for 2-D polycrystals, within the limitations imposed by the slight deviation from a perfectly isotropic response already noted for the "ReX Cu" microstructure, and also (to a lesser extent) in the "Voronoi" case.

## 5. Concluding remarks

In this work, full-field computations have been applied to the case of linearly viscous 2-D polycrystals under antiplane shear. For this case, the numerical implementation of the FFT model has been validated by comparison with an analytical result for the effective properties of incompressible 2-D polycrystals obtained by Lurie and Cherkaev (1984). The examples shown here indicate that the FFT predictions become less accurate as the contrast between single-crystal properties increases.

Different kinds of periodic unit cells were tested with the FFT model. Results on different random configurations of the "tile" microstructure show a relatively high dispersion. In the case of 8-phase polycrystals (built with that low number of phases to try to minimize anisotropic effects) the dispersions were lower but not null, indicating some remaining topological anisotropy. Among these 8-phase microstructures, the distribution of effective properties obtained for different configurations of the numerically generated "Voronoi" microstructure shows less dispersion than the "ReX Cu" case. At this stage, purely numerical aspects cannot be ruled out to explain the better performance of the "Voronoi" microstructure. However, the computation of the 2-point correlation functions for both sets of microstructures clearly indicates that the "Voronoi" microstructure is closer than the "ReX Cu" microstructure to a strict isotropic behavior. In any case, the ensemble averages of polycrystal viscosities, calculated over different random configurations, tend to the theoretical isotropic values, for the three types of microstructures considered.

Concerning local statistics, the stress distributions calculated with the FFT model are asymmetric for a single configuration, and also when ensemble averages are considered. This means that statistical models for polycrystal deformation based on the assumption of Gaussian distributions at local level (e.g. as in Pellegrini, 2000) may lead to inaccurate results. This conclusion, derived here for the case of aggregates with a linear behavior, should apply, even more strongly, to non-linear polycrystals.

As is for the effective properties, the distributions of per-phase first- and second-order moments over different random configurations display some dispersion. In this case, the ensemble averages of the first and second moments of the equivalent stress in the "Voronoi" and "ReX Cu" cases are in good agreement with the corresponding SC estimates for perfectly-disordered microstructures. This means that—at least for the considered cases—the SC estimates for the average field fluctuations are very accurate and only minor effects of the microstructure could be detected.

Finally, it is worth mentioning that the calculation of FFT ensemble averages over random configurations to obtain effective properties, phase averages and field fluctuations, together with the effect of increasing contrast between phases, are further discussed elsewhere, for the more general case of non-linear 2-D (Lebensohn et al., 2004a) and 3-D (Lebensohn et al., 2004b) polycrystals.

## References

Appel, K., Haken, W., 1977. Every planar map is four colorable. Illinois J. Math. 21, 429–567.

Bornert, M., 2001. In: Bornert, M., Bretheau, T., Gilormini, P. (Eds.), Homogénéisation En Mécanique Des Matériaux 1: Matériaux Aléatoires élastiques Et Milieux Périodiques. Hermes Science Publications, Paris, pp. 133–221.

Buryachenko, V.A., Pagano, N.J., Kim, R.Y., Spowart, J.E., 2003. Quantitative description and numerical simulation of random microstructures of composites and their effective elastic moduli. Int. J. Solids Struct. 40, 47–72.

Dykhne, A.M., 1970. Conductivity of a two-dimensional two-phase system. Dokl. Akad. Nauk. SSSR 59, 110–115.

Elvin, A.A., 1996. Number of grains required to homogenize elastic properties of polycrystalline ice. Mech. Mater 22, 51–64.
Hershey, A.V., 1954. The elasticity of an isotropic aggregate of anisotropic cubic crystals. ASME J. Appl. Mech. 21, 236–240.
Kanit, T., Forest, S., Galliet, I., Mounoury, V., Jeulin, D., 2003. Determination of the size of the representative volume element for random composites: statistical and numerical approach. Int. J. Solids Struct. 40, 3647–3679.
Kröner, E., 1958. Berechnung der elastischen Konstanten des Vielkristalls aus den Konstanten des Einkristalls. Z. Physik 151, 504–518.
Kröner, E., 1978. Self-consistent scheme and graded disorder in polycrystal elasticity. J. Phys. F: Met. Phys. 8, 2261–2267.
Kröner, E., 1986. Statistical modelling. In: Gittus, J., Zarka, J. (Eds.), Modelling Small Deformations of Polycrystals. Elsevier, London, pp. 229–291.
Lebensohn, R.A., 2001. N-site modelling of a 3-D viscoplastic polycrystal using the Fast Fourier Transform. Acta Mater. 49, 2723–2737.
Lebensohn, R.A., Liu, Y., Ponte Castañeda, P., 2004a. Macroscopic properties and field fluctuations in model power-law polycrystals: full-field solutions versus self-consistent estimates. Proc. R. Soc. Lond. A 460, 1381–1405.
Lebensohn, R.A., Liu, Y., Ponte Castañeda, P., 2004b. On the accuracy of the self-consistent approximation for polycrystals: comparison with full-field numerical simulations. Acta Mater. 52, 5347–5361.
Liu, Y., Ponte Castañeda, P., 2004a. Second-order theory for the effective behavior and field fluctuations in viscoplastic polycrystals. J. Mech. Phys. Solids 52, 467–495.
Liu, Y., Ponte Castañeda, P., 2004b. Homogenization estimates for the average behavior and field fluctuations in cubic and hexagonal viscoplastic polycrystals. J. Mech. Phys. Solids 52, 1175–1211.
Lurie, K.A., Cherkaev, A.V., 1984. G-closure of some particular sets of admissible material characteristics for the problem of bending of thin elastic plates. J. Optimization Theory Appl. 42, 305–316.
Michel, J., Moulinec, H., Suquet, P., 2000. A computational method based on augmented Lagrangians and Fast Fourier Transforms for composites with high contrast. Comput. Modell. Eng. Sci. 1, 79–88.
Milton, G.W., 2002. The Theory of Composites. Cambridge University Press.
Moulinec, H., Suquet, P., 1994. A fast numerical method for computing the linear and nonlinear properties of composites. C.R. Acad. Sci. Paris II 318, 1417–1423.
Moulinec, H., Suquet, P., 1998. A numerical method for computing the overall response of nonlinear composites with complex microstructure. Comput. Methods Appl. Mech. Eng. 157, 69–94.
Moulinec, H., Suquet, P., 2003. Intraphase strain heterogeneity in nonlinear composites: a computational approach. Eur. J. Mech. A–Solids 22, 751–770.
Nygårds, M., 2003. Number of grains necessary to homogenize elastic materials with cubic symmetry. Mech. Mater. 35, 1049–1057.
Pellegrini, Y.P., 2000. Field distributions and effective-medium approximation for weakly nonlinear media. Phys. Rev. B 61, 9365–9372.
Ponte Castañeda, P., 2002. Second-order homogenization estimates for nonlinear composites incorporating field fluctuations. I—Theory. J. Mech. Phys. Solids 50, 737–757.
Ponte Castañeda, P., Suquet, P., 1998. Nonlinear composites. Adv. Appl. Mech. 34, 171–302.
Ren, Z.Y., Zheng, Q.S., 2002. A quantitative study of minimum sizes of representative volume elements of cubic polycrystals-numerical experiments. J. Mech. Phys. Solids 50, 881–893.
Sab, K., 1992. On the homogenization and the simulation of random materials. Eur. J. Mech. A—Solids 11, 585–607.
Torquato, S., 2002. Random Heterogeneous Materials: Microstructure and Macroscopic Properties. Springer, New York.